Oncology Research, Vol. 28, pp. 605–613
Printed in the USA.

0965-0407/21 $90.00 + .00
DOI: https://doi.org/10.3727/096504020X16022401878096
E-ISSN 1555-3906
www.cognizantcommunication.com

The Usefulness of Pretreatment MR-Based Radiomics on Early Response of Neoadjuvant Chemotherapy in Patients With Locally Advanced Nasopharyngeal Carcinoma

Piao Yongfeng,*†‡§[1] Jiang Chuner,*¶#[1] Wang Lei,*†‡§ Yan Fengqin,*†‡§ Ye Zhimin,*†‡§ Fu Zhenfu,*†‡§ Jiang Haitao,*·**†† Jiang Yangming,‡‡ and Wang Fangzheng*†‡§

*Department of Radiation Oncology, Cancer Hospital of the University of Chinese Academy of Sciences (Zhejiang Cancer Hospital), Zhejiang, P.R. China
†Institute of Cancer and Basic Medicine (ICBM), Chinese Academy of Sciences, Zhejiang, P.R. China
‡Key Laboratory of Head Neck Cancer of Zhejiang Province, Zhejiang Cancer Hospital, Zhejiang, P.R. China
§Key Laboratory of Radiation Oncology of Zhejiang Province, Zhejiang, P.R. China
¶Department of Breast Tumor Surgery, Cancer Hospital of the University of Chinese Academy of Sciences, Zhejiang, P.R. China
#Department of Breast Tumor Surgery, Zhejiang Cancer Hospital, Zhejiang, P.R. China
**Department of Radiology, Cancer Hospital of the University of Chinese Academy of Sciences, Zhejiang, P.R. China
††Department of Radiology, Zhejiang Cancer Hospital, Zhejiang, P.R. China
‡‡Department of Digital Earth, Institute of Remote Sensing and Digital Earth, CAS, Beijing, P.R. China

The aim of this study was to explore the predictive role of pretreatment MRI-based radiomics on early response of neoadjuvant chemotherapy (NAC) in locoregionally advanced nasopharyngeal carcinoma (NPC) patients. Between January 2016 and December 2016, a total of 108 newly diagnosed NPC patients who were hospitalized in the Cancer Hospital of the University of Chinese Academy of Sciences were reviewed. All patients had complete data of enhanced MR of nasopharynx before treatment, and then received two to three cycles of TP-based NAC. After 2 cycles of NAC, enhanced MR of nasopharynx was conducted again. Compared with the enhanced MR images before treatment, the response after NAC was evaluated. According to the evaluation criteria of RECIST1.1, 108 cases were divided into two groups: 52 cases for the NAC-sensitive group and 56 cases for the NAC-resistance group. ITK-SNAP software was used to manually sketch and segment the region of interest (ROI) of nasopharyngeal tumor on the MR enhanced T1WI sequence image. The parameters were analyzed and extracted by using AI Kit software. ANOVA/MW test, correlation analysis, and LASSO were used to select texture features. We used multivariate logistic regressions to select texture features and establish a predictive model. The ROC curve was used to evaluate the efficiency of the predictive model. A total of 396 texture features were obtained by using feature calculation. After all features were screened, we selected two features including ClusterShade_angle135_offset4 and Correlation_AllDirection_offshe1_SD. Based on these two features, we established a predictive model by using multivariate logistic regression. The AUC of the two features used alone (0.804, 95% CI = 0.602–0.932; 0.762, 95% CI = 0.556–0.905) was smaller than the combination of these two features (0.905, 95% CI = 0.724–0.984, $p = 0.0005$). Moreover, the sensitivity values of the two features used alone and the combined use were 92.9%, 51.7%, and 85.7%, respectively, while the specificity values were 66.7%, 91.7%, and 83.3%, respectively, in the early response of NAC for NPC. The predictive model based on MRI-enhanced sequence imaging could distinguish the sensitivity and resistance to NAC and provide new biomarkers for the early prediction of the curative effect in NPC patients.

Key words: Nasopharyngeal carcinoma (NPC); Neoadjuvant chemotherapy (NAC); Response prediction; Magnetic resonance imaging (MRI); Radiomics; Texture analysis

[1]These authors provided equal contribution to this work.

Address correspondence to Wang Fangzheng, Department of Radiation Oncology, Cancer Hospital of the University of Chinese Academy of Sciences, No. 1, Banshan East Road, Hangzhou, Zhejiang 310022, P.R. China. Tel: 86-571-88128192; E-mail: wangfz76@126.com *or* Jiang Haitao, Department of Radiology, Cancer Hospital of the University of Chinese Academy of Sciences, Zhejiang, Hangzhou 310022, P.R. China. Tel: 86-571-88128192; E-mail: jianght@zjcc.org.cn

INTRODUCTION

Nasopharyngeal cancer (NPC) is a unique malignancy of the head and neck for which incidence is 15–50 cases per 100,000 annually in endemic areas such as Southeast Asia, northern Africa, and middle Europe[1]. The GLOBOCAN data[2] in 2018 reported that 129,097 patients were newly diagnosed with NPC worldwide. Of these patients, 47.7% occurred in China. Because of the high sensitivity to radiation and the complicated anatomical structure of the nasopharynx, radiation therapy (RT) is regarded as the mainstay of treatment for NPC. Unfortunately, the proportion of locally advanced NPC at diagnosis is approximately 60%–70%[3]. The combination of RT and chemotherapy was used to treat NPC. In a series of meta-analysis and clinical trails, concurrent chemotherapy (CC) has always played a very important role in the treatment of NPC[4,5], while adjuvant chemotherapy (AC) did not provide survival benefits for locoregionally advanced NPC patients receiving less than three cycles of AC[6]. Because of the introduction of magnetic resonance imaging (MRI) and neoadjuvant chemotherapy (NAC), the survival of patients with locoregionally advanced NPC has improved continually. Moreover, NAC can improve patients' tolerability, eradicate micrometastases, and protect normal tissue due to the reduction of tumor compared with AC[7]. Several studies demonstrated that additional NAC to the standard treatment provided survival advantages for locoregionally advanced NPC[8–11]. Thus, additional NAC followed by concurrent chemoradiotherapy (CCRT) was recommended as first-line strategy for locoregionally advanced NPC by the 2019 National Comprehensive Cancer Network (NCCN) guideline. Although adding NAC prior to CCRT significantly increased local control and reduced distant metastasis, favorable response to NAC was not observed in all patients with locoregionally advanced NPC, as only less than 50% of these patients were sensitive to NAC[12,13]. Moreover, the response of NAC was associated with the survival outcomes of the patients with locoregionally advanced NPC[13,14]. Peng et al. showed that the response to NAC was the independent prognostic factor of disease-free survival (DFS), overall survival (OS), and locoregional recurrence-free survival (LRRFS) at 4 years[13]. Liu et al. indicated that the resistance to NAC was a poor prognostic factor of locoregionally advanced NPC[14]. However, the effective biomarkers were lacking to predict the early response of NAC for locoregionally advanced NPC patients.

In 2012, Lambin et al.[15] first proposed the concept of radiomics, which aimed to extract a large number of quantitative parameters through the machine learning method to evaluate tumor heterogeneity. Previous studies had shown that radiomics could reflect the tumor heterogeneity and the information on genetic level and show a favorable predictive role in gene mutation, curative effect, and prognosis[16–18]. Most of the studies used diffusion-weighted MRI to predict and evaluate the therapeutic effects in NPC patients[19–21]. However, the application of these markers in the prediction of the therapeutic effects of NAC in NPC patients remains controversial. Recently, some research applied radiomics based on magnetic resonance (MR) images to predict the response of RT and chemotherapy, and explore the relationship between tumor response and survival in NPC patients[22–25]. The aims of this study were to explore the correlation between the texture features based on pretreatment MR images and early response of NAC and to reveal the feasibility of radiomics in predicting early response of NAC in NPC patients.

MATERIALS AND METHODS

Patients

Between January 2016 and December 2016, 108 patients hospitalized in the Department of Radiation Oncology at Zhejiang Cancer Hospital were retrospectively reviewed. Eligible patients met the following criteria: (i) biopsy-proven NPC, (ii) no metastasis occurred, (iii) received two to three cycles of NAC, (iv) had complete data of MRI pre- and post-NAC, (v) had a measurable lesion in pre-NAC MRI of nasopharynx, and (v) no previous anticancer treatment. Patients who refused NAC, did not complete NAC, had any metastasis at diagnosis, or had previous anticancer treatment were excluded. This retrospective study was approved by the Medical Ethics Committee and the institutional reviewed board of Zhejiang Cancer Hospital. All treatment protocols in this study were carried out in accordance with NCCN guidelines. Because of the retrospective design of the study, the committee confirmed that informed consent was not required.

Pretreatment Evaluations

Pretreatment evaluations included the following: detailed medical histories, an evaluation of performance status (PS), and careful physical examination. MRIs of the nasopharynx and nasopharyngoscopies were performed. Chest computed tomography (CT), bone scans, abdominal ultrasound, and hematology and biochemistry profiles were conducted 1 week before treatment. Positron emission tomography (PET) scans and abdominal CT scans were performed as clinically indicated. The 2010 American Joint Committee on Cancer (AJCC) staging system and World Health Organization (WHO) classification were recommended to be used in this study. We were blinded to other information.

Chemotherapy

All NPC patients enrolled into the present study were given three weekly docetaxel plus cisplatin-based

NAC, and three weekly CC with cisplatin. The available TP-based NAC regimens included docetaxel 60 mg/m^2/day on day 1 and cisplatin 25 mg/m^2/day on days 1 to 3. Two to three cycles of NAC were administrated.

Evaluation of Response to NAC and Group

With 3 weeks after two cycles of NAC, MR examination of the nasopharynx and nasopharyngoscopy were performed again. Compared with the baseline nasopharyngeal MR images and nasopharyngoscopy, the response to NAC was only evaluated using the reduction in primary measurable tumor. According to the RECIST 1.1 standard to evaluate the efficacy[26], complete remission (CR) is defined as the disappearance of target lesion (short radius of retropharyngeal lymph nodes: <5 mm); partial remission (PR) is defined as a reduction of at least 30% in the sum of the longest diameter of target lesions compared with the baseline sum longest diameter before treatment; partial progression (PD) is defined as an increase of at least 20% in the sum of the longest diameter of target lesions (using smallest sum longest diameter since treatment started or appearance of one or more new lesions as reference); and stable (SD) is defined as neither sufficient shrinkage to qualify for PR nor sufficient increase to qualify for PD (using smallest sum longest diameter since treatment started as reference). After two cycles of NAC, 52 patients who evaluated as PR or CR were enrolled into the sensitive group, and 56 patients who were assessed as SD or PD were included in the resistance group.

MR Image Scanning Scheme

The contrast-enhanced (CE) MR examinations of the nasopharynx and cervical region were conducted pre- and post-NAC by using head and neck coils with 3.0-T MR scanners (Verio3.0T, Siemens Medical Solutions, Germany). Before contrast was performed, we obtained the MR images including T1-weighted fast spin-echo images in the axial plane, T2-weighted fast spin-echo MR images in the axial plane, and T2-weighted fat-suppressed spin-echo sequence. The scanning parameters included T1-weighted fast spin-echo images [repetition time (TR) = 450 ms; echo time (TE) = 8.8 ms, flip angle = 90°, matrix = 256 × 168, slice thickness = 4 mm, spacing between slices = 0.8 mm), T2-weighted fast spin-echo images (TR = 6,000 ms, TE = 95 ms, flip angle = 90°, matrix = 256 × 168, slice thickness = 4 mm, spacing between slices = 0.8 mm), and T2-weighted fat-suppressed spin-echo images (TR = 6,360 ms, TE = 95 ms, flip angle = 90°, matrix = 256 × 168, slice thickness = 4 mm, spacing between slices = 0.8 mm). The intravenous injections of 15 ml contrast agent (Ounaiying, 0.5 mmol/ml) and 15 ml saline were performed at a rate of 1.5 ml/s. After 20 s, the axial T1-weighted fast spin-echo sequence was administrated with the same parameters as those of T1-weighted fast spin-echo images in the axial plane.

Analysis of Radiomics Based on MR Images

Image Segmentation. We searched the MR images of the nasopharynx before NAC from PACS at the Cancer Hospital of the University of Chinese Academy of Sciences and saved as DICOM format images for each patient. Then the DICOM format images of the CE T1WI sequence were imported into the ITK-SNAP software (version 3.8.0 for Mac, http://www.itksnap.org/). After consultation, two deputy chief radiologists experienced in MRI diagnosis of NPC selected the largest primary tumor cross-sectional area from the CE T1-weighted images of the nasopharynx (Fig. 1A) and manually delineated a ROI around the entire heterogeneous enhanced tumor outline (Fig. 1B). Large blood vessels such as the carotid artery, bleeding, and necrotic cystic areas were avoided to be included in the ROI. Then the single-layer tumor image was segmented (Fig. 1C).

Extraction of Texture Features and Preprocessing. A total of 108 ROI images segmented from pre-NAC CE T1W1 MR images of the nasopharynx were extracted by using artificial intelligence kit software (AI Kit V3.0.0.R,

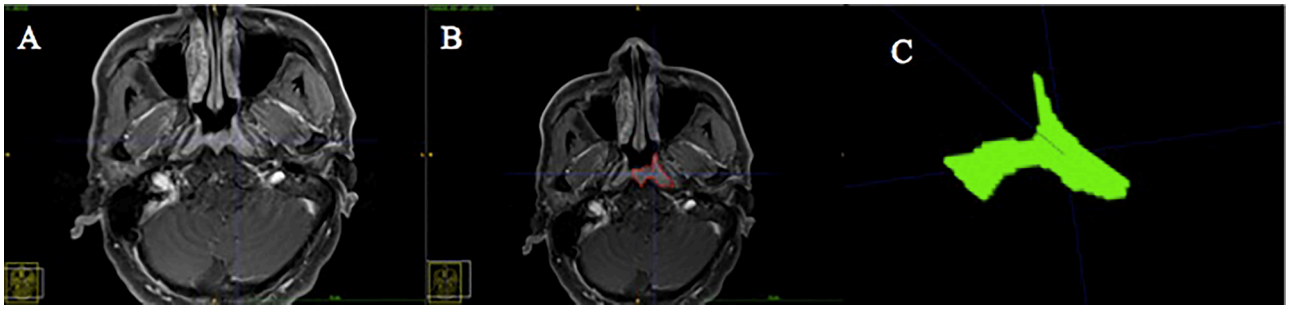

Figure 1. Magnetic resonance (MR) image segmentation and the delineation of region of interest (ROI). (A) The largest primary tumor cross-sectional area in the CE T1-weighted images of the nasopharynx. (B) Delineation of an ROI around the entire heterogeneous enhanced tumor outline. (C) ROI in the segmented single-layer tumor image.

GE Healthcare). There are five kinds of calculation methods of texture features including first-order statistical features, second-order texture features, gray-level co-occurrence matrix (GLCM), gray-level gradient co-occurrence matrix (GLGCM), and wavelet transform. A total of 396 imaging features were extracted in each patient before feature selection, including 42 first-order statistical features, 21 second-order texture features, 153 GLCM features, 154 GLGCM features, and 26 wavelet transform features. In order to ensure the comparability among the data, the data of different orders of magnitude were converted to the same order of magnitude. The data preprocessing steps are as follows: 1) the singular value was replaced by median value; 2) each texture feature was standardized by a *Z*-score, and the calculation formula was as follows [(parameter value − mean value)/standard deviation; μ, mean value; σ, standard deviation; *N*, the number of cases]:

$$\sigma = \sqrt{\frac{1}{N}\sum_{i=1}^{N}(x_i - \mu)^2} \qquad z = \frac{x - \mu}{\sigma}$$

Statistical Analysis

SPSS 22.0 software was used to analyze the general data of patients. We used the chi-square test to compare the baseline characteristics between sensitive and resistance groups. When the values were $p < 0.05$, the differences were statistically significant.

The extracted 396 parameters were divided into five categories. If all these parameters were evaluated together, it would cause overfitting. Moreover, irrelevant and redundant parameters would confuse the learning algorithm. Therefore, R language (https://www.r-project.org/) was used for statistical analysis.

The preprocessing before feature selection was divided into three steps. At the first step, the AI Kit software sought to identify the features, and the analysis of variance (ANOVA)/Mann–Whitney (MWA) *U*-test was used to select the features. At the second step, the correlation analysis reduced the dimension. The filter threshold was set to 0.9 for the Spearman rank correlation coefficient analysis. At the third step, the least absolute shrinkage and selection operator (LASSO) Cox regression model were used to screen out the features.

The selected features were used to conduct the predictive model using multiple logistic regression analysis according to early response of NAC. The receiver operating characteristic curve (ROC) was drawn, and the area under the curve (AUC) was calculated. The interactive point map was drawn and provided the boundary value, sensitivity, and specificity between the two groups.

RESULTS

Patient Characteristics

From January 2016 to December 2016, a total of 108 eligible patients with NPC were enrolled into the present study. According to the early response of NAC, 52 patients were assigned to the sensitive group and 56 cases to the resistance group. Table 1 lists the baseline demographic of patients and tumor characteristics. The basic characteristics of patients were well balanced between two groups.

Features Selection

A total of 396 features were extracted from CE T1W1 MR images by using the AI Kit software. The selective

Table 1. Basic Characteristics of 108 Nasopharyngeal Carcinoma (NPC) Patients Between the Sensitive and Resistant Groups

Characteristics	Total (*N* = 108)	Sensitive Group (*N* = 52)	Resistant Group (*N* = 56)	*p* Value
Age [mean (range)]	54 (22–70)	54 (39–68)	51 (22–70)	0.836
<60 years	52	24	28	
≥60 years	56	28	28	
Gender				0.666
Male	80	40	40	
Female	28	12	16	
T stage				0.734
T1–2	36	16	20	
T3–4	18	36	36	
N stage				0.924
N0–2	68	32	36	
N3	40	20	20	
Clinical stage				0.312
III	48	20	28	
IV	60	32	28	

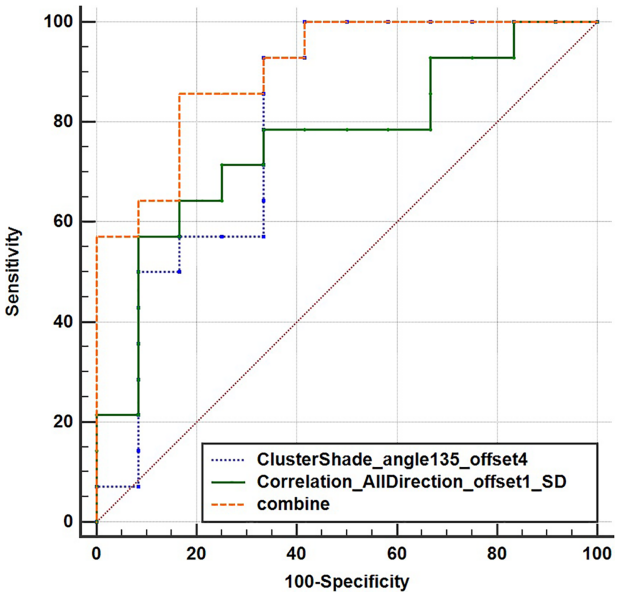

Figure 2. ROC curves of two texture feature used alone or in combination to nasopharyngeal carcinoma.

method was ANOVA + MW test. After ANOVA and MW test, 14 features remained. Then the selective method was the correlation analysis, and the remaining feature number was 7. Last, the selective method was LASSO. The threshold value was 0.9, and the remaining feature number was 2. The two features included ClusterShade_angle 135_offset 4 and Correlation_AllDirection_offshel_SD.

Predictive Efficacy of Two Characteristic Parameters Used Alone or in Combination to NPC

Then the two texture features were used to conduct the predictive model through multiple logistic regression analysis according to early response of NAC. The indicators such as AUC, sensitivity, specificity, and cut-off value expressed the value of these features to predict early response of NAC. We drew ROC and calculated AUC values (Fig. 2). As shown in Figure 2 and Table 2, the AUC value of ClusterShade_angle 135_offset 4 [0.804, 95% confidence interval (CI) = 0.602–0.932] or Correlation_AllDirection_offshel_SD (0.762, 95% CI = 0.556–0.905) used alone was smaller than the combination of these two parameters (0.905, 95% CI = 0.724–0.984, p = 0.0005). Moreover, the sensitivity values of the two parameters used alone and the combined use were 92.9%, 51.7%, and 85.7%, respectively, while the specific values were 66.7%, 91.7%, and 83.3%, respectively, in the early response of NAC for NPC (Table 2 and Fig. 3). In addition, the cut-off values of the two features used alone and the combined use were –0.1116, 0.1356 and 0.4535, respectively (Fig. 3, Table 3).

DISCUSSION

Because resistance to NAC is a poor prognostic factor for locoregionally advanced NPC, early response predictions are very important to select therapeutic regimens and modify treatment planning. Currently, no available biomarkers are used to predict the response of NAC before treatment. Here we delineated the ROI on the pre-NAC CE T1W1 MR images and extracted 396 texture features using AI Kit software. The two features such as ClusterShade_angle 135_offset 4 and Correlation_AllDirection_offshel_SD were screened out and used to perform a predictive model through multiple logistic regression analyses. Subsequently, the ROC and AUC values were calculated. The AUC value of the combined two features (0.905, 95% CI = 0.724–0.984) was greater than two features used alone (0.804, 95% CI = 0.602–0.932; 0.762, 95% CI = 0.556–0.905, p = 0.0005). Moreover, the sensitivity values of the two features used alone and the combined use were 92.9%, 51.7%, and 85.7%, respectively, while the specific values were 66.7%, 91.7%, and 83.3%, respectively, in the early response of NAC for NPC. In addition, the cut-off values of the two features used alone and the combined use were –0.1116, 0.1356, and 0.4535, respectively (Fig. 3). Therefore, radiomics features based on the pretreatment provided favorable predictive biomarkers for early response to NAC in locoregionally NPC patients.

Because tumor response was used as an independent predictor, it is of great clinical value to predict the sensitivity of NAC in patients with NPC before treatment. Dou et al. indicated that survival rate in NPC patients with CR tumor response was 75.5%[26]. Feryel et al. found that the patients with PR tumor response obtained a survival rate of 54.2%[27]. Peng et al. revealed that survival rates in patients with CR, PR, and PD tumor responses were 90%, 79%, and 58.2%, respectively[13]. Dwijayanti et al. performed a retrospective study to determine the survival outcomes based on treatment response. The results indicated that 5-year survival rates of NPC patients with CR,

Table 2. Logistic Regression Analyses of Texture Feature Parameters on Early Response of Neoadjuvant Chemotherapy (NAC) in NPC Patients

Variable	*B*	SE	Wald	OR	95% CI	*p* Value
ClusterShade_angle 135_offset 4	1.35624	0.66113	4.2082	3.8816	1.0623–14.1832	0.0402
Correlation_AllDirection_offshel_SD	1.98007	0.98203	4.0654	7.2432	1.0568–49.6428	0.0438

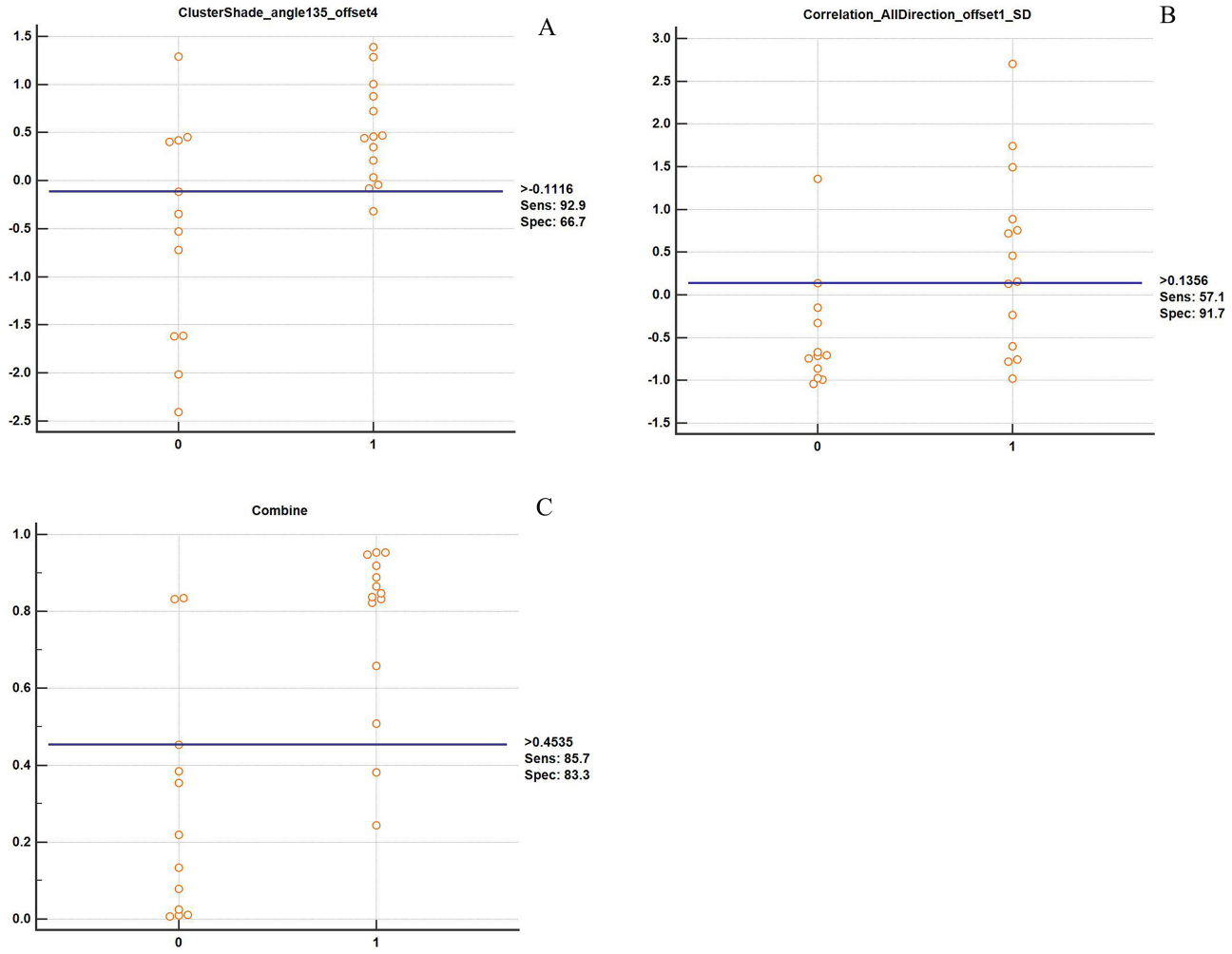

Figure 3. Correlative analysis of texture features and early response of neoadjuvant chemotherapy (NAC). (A) ClusterShade_angle 135_offset 4. (B) Correlation_AllDirection_offshel_SD. (C) The combination of two features.

PR, and PD were 71%, 30.4%, and 10.6%, respectively[28]. Peng et al. showed that the response to NAC was the independent prognostic factors of DFS, OS, and LRRFS at 4 years[13]. In contrast, unsatisfactory response of NAC was associated with poor survival outcomes including LRRFS and PFS in locoregionally advanced NPC patients[29]. Liu et al. also indicated that the resistance to NAC was a poor prognostic factor of locoregionally advanced NPC[14]. Because of resistance to NAC, the patients had the excess economic burden and experienced more toxicities and delays in the implementation of later therapy. Thus, we explored the effective biomarkers to select appropriate strategy before treatment.

Currently, the early response of NAC in NPC patients was predicted by using more than three imaging modalities including intravoxel incoherent motion diffusion-weighted MR imaging (IVIM-DWI)[30,31], dynamic CE MR imaging (DCE-MRI)[32,33], and diffusion-weighted MR imaging (DWI)[34,35]. However, the predictive efficacy of SWI and DCE-MRI for early response of NAC remained controversial. In addition, the IVIM-DWI-based pure diffusion coefficient values were used to

Table 3. The Value of Two Feature Parameters Used Alone or in Combination to Nasopharyngeal Carcinoma

Parameters	Cutoff Value	Sensitivity	Specificity	AUC
ClusterShade_angle 135_offset 4	–0.1116	92.9	66.7	0.804 (95% CI = 0.602–0.932)
Correlation_AllDirection_offshel_SD	0.1356	51.7	91.7	0.762 (95%CI = 0.556–0.905)
Combined two parameters	0.4535	85.7	83.3	0.905 (95%CI = 0.724–0.984)

assess the response to NAC, and the results showed that the sensitivity and specificity were 0.647–0.658 and 0.722–0.818, respectively[30,31]. Thus, these studies indicated that the specificity values were low. MRI-based radiomics was used to predict pathological response, survival, and prognosis for solid tumors such as rectal cancer[16], breast cancer[36], and lung cancer[17,18]. Based on MR images, radiomics was used to predict the response to chemoradiotherapy for NPC[23]. Zhao et al. used multiparametric MRI-based radiomics to assess response of NAC, and their findings demonstrated that 3-year PFS in patients with sensitivity to NAC was better than that in patients with resistance to NAC (84.81% vs. 39.75%, $p < 0.001$)[37]. Wang et al. extracted five features from CE T1W1 MR images, and the AUC value was 0.715 with sensitivity of 0.94 and specificity of 0.500[24]. Thus, we extracted two texture features from CE T1W1 MR images and used them to predict early response to NAC. These findings indicated that the sensitivity values of the two features used alone and the combined use were 92.9%, 51.7%, and 85.7%, respectively, while the specific values were 66.7%, 91.7%, and 83.3%, respectively, in the early response of NAC for NPC.

The texture features of radiomics are the mathematical measurement values calculated according to voxel arrangement. They can represent the heterogeneity of voxel arrangement in tumor space[38]. Tumor heterogeneity may be associated with tumor cell proliferation, angiogenesis, and necrosis, and even reflect the information at the genetic level in a certain degree[39]. Through the arrangement of voxels in tumor space, the radiomics based on MR images can reflect the tumor heterogeneity, which was related to the efficacy and prognosis. Two texture features from pretreatment CE T1W1 MR images in this study included ClusterShade_angle 135_offset 4 and Correlation_AllDirection_offshel_SD. The first mentioned of two described the surface condition of the tumor such as smooth or rough, while the latter belonged to the gray symbiotic matrix and had directionality. It reflected the similarity and symmetry of the distribution of different gray pixels in the images as well as the spatial position relationship between the pixels. Moreover, it also reflected the difference of the internal details of the tumor, which is an important factor affecting the therapeutic effect of NAC.

Several studies had shown that three-dimensional analysis could more completely reflect the heterogeneity of tumor tissue[40]. However, three-dimensional analysis was more complex and time-consuming. Because the thickness of the MRI layer was 4 mm, the edge part would be affected by partial volume effect, and it was difficult to grasp the lesion border when manually sketching lesions in the head and tail direction. A study performed by Lubner et al. showed that there was no statistically significant difference between the three-dimensional analysis and two-dimensional analysis, and the results based on single-layer and two-dimensional ROI analysis were reliable[41]. Therefore, the single-layer and two-dimensional ROI analyses were used in the present study.

Although this study provides the predictive role of early response of NAC in locoregionally advanced NPC patients, several limitations were observed in this study. First, the sample size is small and a validation group was not used to assess this model. Second, the study was conducted using a single MR scanning instrument in a single-center study, and it failed to distinguish the prediction efficiency of different MR scanners in different centers. In addition, we assess the tumor response through volumetric changes between pre- and post-NAC based on RECIST 1.1, but this evaluation was insufficient due to lack of molecular events.

CONCLUSION

In conclusion, the current study screened out two texture features based on pretreatment CE T1W1 MR images and established a predictive model for early response of NAC. Moreover, we proved that this model could well predict the sensitivity of NAC in NPC patients. As a predictive biomarker of early response of NAC, radiomics based on pretreatment MR can provide a new method to predict the therapeutic effect of NAC and guide the individualized treatment for NPC patients. It needs to expand the sample size and perform multicenter prospective research to verify the predictive model.

ACKNOWLEDGMENTS: This study was supported by grants from the Medical and Health Science and Technology Program of Zhejiang Province (Nos. 020KY084, 2019KY041, 2013KYB033, 2009B026, 2006A016, 2005B012, and 2004B014) and National Natural Science Foundation of China (No. 81502647). Author contributions: conception and design: Fangzheng Wang, Haitao Jiang, Zhenfu Fu, and Yangming Jiang; acquisition of data: Chuner Jiang, Lei Wang, Fengqin Yan, Zhimin Ye, and Yongfeng Piao; Data analysis and interpretation: Fangzheng Wang and Yangming Jiang; drafting the article and revising it critically for important intellectual content: Yongfeng Piao, Fangzheng Wang, Zhenfu Fu, and Yangming Jiang; final approval of manuscript: all authors. The authors declare no conflicts of interest.

REFERENCES

1. Tang LL, Chen WQ, Xue WQ, He YQ, Zheng RS, Zeng YX, Jia WH. Global trends in incidence and mortality of nasopharyngeal carcinoma. Cancer Lett. 2016;374(1):22–30.
2. Bray F, Ferlay J, Soerjomataram I, Siegel RL, Torre LA, Jemal A. Global cancer statistics 2018: GLOBOCAN estimates of incidence and mortality worldwide for 36 cancers in 185 countries. CA Cancer J Clin. 2018;68(6):394–424.
3. Chen L, Mao YP, Xie FY, Liu LZ, Sun Y, Tian L, Tang LL, Lin AH, Ma J. The seventh edition of UICC/AJCC staging system for nasopharyngeal carcinoma is prognostically useful for patients treated with intensity-modulated radiotherapy from an endemic area in China. Radiother Oncol. 2012;104(3):331–7.

4. Al-Sarraf M, LeBlanc M, Giri PG, Fu KK, Cooper J, Vuong T, Forastiere AA, Adams G, Sakr WA, Schuller DE, Ensley JF. Chemoradiotherapy versus radiotherapy in patients with advanced nasopharyngeal cancer: Phase III randomized intergroup study 0099. J Clin Oncol. 1998;16(4):1310–7.
5. Lee AW, Tung SY, Chua DT, Ngan RK, Chappell R, Tung R, Siu L, Ng WT, Sze WK, Au GK, Law SC, O'Sullivan B, Yau Tk, Leung TW, Au JS, Sze WM, Choi CW, Fung KK, Lau JT, Lau WH. Randomized trial of radiotherapy plus concurrent-adjuvant chemotherapy vs radiotherapy alone for regionally advanced nasopharyngeal carcinoma. J Natl Cancer Inst. 2010;102(15):1188–98.
6. Chen L, Hu CS, Chen XZ, Hu GQ, Cheng ZB, Sun Y, Li WX, Chen YY, Xie YF, Liang SB, Chen Y, Xu TT, Li B, Long GX, Wang SY, Zheng BM, Guo Y, Sun Y, Mao YP, Tang LL, Chen YM, Liu MZ, Ma J. Concurrent chemoradiotherapy plus adjuvant chemotherapy versus concurrent chemoradiotherapy alone in patients with locoregionally advanced nasopharyngeal carcinoma: A phase 3 multicentre randomised controlled trial. Lancet Oncol. 2012;13(2):163–71.
7. Sun Y, Li WF, Chen NY, Zhang N, Hu GQ, Xie FY, Sun Y, Chen XZ, Li JG, Zhu XD, Hu CS, Xu XY, Chen YY, Hu WH, Guo L, Mo HY, Chen L, Mao YP, Sun R, Ai P, Liang SB, Long GX, Zheng BM, Feng XL, Gong XC, Li L, Shen CY, Xu JY, Guo Y, Chen YM, Zhang F, Lin L, Tang LL, Liu MZ, Ma J. Induction chemotherapy plus concurrent chemotherapy versus concurrent chemoradiotherapy alone in locoregionally advanced nasopharyngeal carcinoma: A phase 3, multicentre, randomized controlled trial. Lancet Oncol. 2016;17(11):1509–20.
8. Hui EP, Ma BB, Leung SF, King AD, Mo F, Kam MK, Yu BK, Chiu SK, Kwan WH, Ho R, Chan I, Ahuja AT, Zee BC, Chan AT. Randomized phase II trial of concurrent cisplatin-radiotherapy with or without neoadjuvant docetaxel and cisplatin in advanced nasopharyngeal carcinoma. J Clin Oncol. 2009;27(2):242–9.
9. Fangzheng W, Chuner J, Lei W, Fengqin Y, Zhimin Y, Quanquan S, Tongxin L, Min X, Peng X, Bin L, Aizawa R, Sakamoto M, Zhenfu F. Addition of 5-fluorouracil to first-line induction chemotherapy with docetaxel and cisplatin before concurrent chemoradiotherapy does not improve survival in locoregionally advanced nasopharyngeal carcinoma. Oncotarget 2017;8(53):91150–61.
10. Fangzheng W, Quanquan S,Chuner J, Lei W, Fengqin Y, Zhimin Y, Tongxin L, Min X, Peng X, Haitao J, Aizawa R, Sakamoto M, Yuezhen W, Zhenfu F. Gemcitabine/cisplatin induction chemotherapy before concurrent chemotherapy and intensity-modulated radiotherapy improves outcomes for locoregionally advanced nasopharyngeal carcinoma. Oncotarget 2017;8(57):96798–7808.
11. Zhang Y, Chen L, Hu GQ, Zhang N, Zhu XD, Yang KY, Jin F, Shi M, Chen YP, Hu WH, Cheng ZB, Wang SY, Tian Y, Wang XC, Sun Y, Li JG, Li WF, Li YH, Tang LL, Mao YP, Zhou GQ, Sun R, Liu X, Guo R, Long GX, Liang SQ, Li L, Huang J, Long JH, Zang J, Liu QD, Zou L, Su QF, Zheng BM, Xiao Y, Guo Y, Han F, Mo HY, LV JW, Du XJ, Xu C, Liu N, Li YQ, Chua MLK, Xie FY, Sun Y, Ma J. Gemitabine and cisplatin induction chemotherapy in nasopharyngeal carcinoma. N Eng l J Med. 2019;381(12):1124–35.
12. Yen RF, Chen TH, Ting LL, Tzen KY, Pan MH, Hong RL. Early restaging whole-body (18)F-FDG PET during induction chemotherapy predicts clinical outcome in patients with locoregionally advanced nasopharyngeal carcinoma. Eur J Nucl Med Mol Imaging 2005;32(10):1152–9.
13. Peng H, Chen L, Zhang Y, Li WF, Mao YP, Liu X, Zhang F, Guo R, Liu LZ, Tian L, Lin AH, Sun Y, Ma J. The tumor response to induction chemotherapy has prognostic value for long-term survival outcomes after intensity-modulated radiation therapy in nasopharyngeal carcinoma. Sci Rep. 2016;6:24835.
14. Liu LT, Tang LQ, Chen QY, Zhang L, Guo SS, Guo L, Mo HY, Zhao C, Guo X, Cao KJ, Qian CN, Zeng MS, Bei JX, Hong MH, Shao JY, Sun Y, Ma J, Mai HQ. The prognostic value of plasma Epstein–Barr viral DNA and tumor response to neoadjuvant chemotherapy in advanced-stage nasopharyngeal carcinoma. Int J Radiat Oncol Biol Phys. 2015;93(4):862–9.
15. Lambin P, Rios-Velazquez E, Leijenaar R, Carvalho S, van Stiphout RG, Granton P, Zegers CM, Gillies R, Boellard R, Dekker A, Aerts HJ. Radiomics: Extracting more information from medical images using advanced feature analysis. Eur J Cancer 2012;48(4):441–6.
16. Nie K, Shi L, Chen Q, Hu X, Jabbour SK, Yue N, Niu TY, Sun XN. Rectal cancer: Assessment of neoadjuvant chemoradiation outcome based on radiomics of multiparametric MRI. Clin Cancer Res. 2016;22(21):5256–64.
17. Zhu XZ, Dong D, Chen ZD, Fang MJ, Zhang LW, Song JD, Yu DD, Zang YL, Liu ZY, Shi JY, Tian J. Radiomic signature as a diagnostic factor for histologic subtype classification of non-small cell lung cancer. Eur Radiol. 2018;28(7):2772–8.
18. Li YJ, Lu L, Xiao MJ, Dercle L, Huang Y, Zhang ZS, Schwartz LH, Li DQ, Zhao BS. CT slice thickness and convolution kernel affect performance of a radiomic model for predicting EGFR status in non-small cell lung cancer: A preliminary study. Sci Rep. 2018;8(1):17913.
19. Law BKH, King AD, Bhatia KS, Ahuja AT, Kam MKM, Ma BB, Ai QY, Mo FKF, Yuan J, Yeung DKW. Diffusion-weighted imaging of nasopharyngeal carcinoma: Can pretreatment DWI predict local failure based on long-term outcome? AJNR 2016;37(9):36–43.
20. Huang WY, Li MM, Lin SM, Chen F, Yang K, Zhu XL, Wu Gang, Li JJ. In vivo imaging markers for prediction of radiotherapy response in patients with nasopharyngeal carcinoma: RESOLVE DWI versus DKI. Sci Rep. 2018;8(1):15861.
21. Song CR, Cheng P, Cheng JL, Zhang Y, Sun MT, Xie SS, Zhang XN. Differential diagnosis of nasopharyngeal carcinoma and nasopharyngeal lymphoma based on DCE-MRI and RESOLVE-DWI. Eur Radiol. 2020;30(1):110–8.
22. Liu J, Mao Y, Li ZJ, Zhang DK, Zhang ZC, Hao SN, Li BS. Use of texture analysis based on contrast-enhanced MRI to predict treatment response to chemoradiotherapy in nasopharyngeal carcinoma. J Magn Reson Imaging 2016;44(2):445–55.
23. Zhang B, Tian J, Dong D, Gu DS, Dong YH, Zhang L, Lian ZY, Liu J, Luo XN, Pei SF, Mo XK, Huang WH, Quyang FS, Guo BL, Liang L, Chen WB, Liang CH, Zhang SX. Radiomics features of multiparametric MRI as novel prognostic factors in advanced nasopharyngeal carcinoma. Clin Cancer Res. 2017;23(15):4259–69.
24. Wang GY, He L, Yuan C, Huang YQ, Liu ZY, Liang CH. Pretreatment MR imaging radiomics signatures for response prediction to induction chemotherapy in patients with nasopharyngeal carcinoma. Eur J Radiol. 2018;98:100–6.
25. Eisenhauer EA, Therasse P, Bogaerts J, Schwartz LH, Sargent D, Ford R, Dancey J, Arbuck S, Gwyther S, Mooney M, Rubinstein L, Shankar L, Dodd L, Kaplan R, Lacombe D, Verweij J. New response evaluation criteria in

solid tumors: Revised RECIST guideline (version 1.1). Eur J Cancer 2009;45(2):228–47.
26. Dou H, Hu D, Lam C, Liu Y, Wang X, Zhang W. Retrospective analysis of results of treatment for nasopharyngeal carcinoma in Macao. Chin J Cancer Res. 2014;26(2):148–58.
27. Feryel L, Yosra B, Mouna A. Complete clinical response after induction chemotherapy followed by chemoradiotherapy in nasopharyngeal carcinoma: Impact on oncologic outcomes. Int J Otorhinolaryngol Head Neck Surg. 2018;2(1):1–5.
28. Dwijayanti F, Prabawa A, Besral, Cita H. The five-year survival rate of patients with nasopharyngeal carcinoma based on tumor response after receiving neoadjuvant chemotherapy, followed by chemoradiation in Indonesia: A retrospective study. Oncology 2020;98(3):154–60.
29. Tabuchi K, Nakayama M, Nishimura B, Hayshi K, Hara A. Early detection of nasopharyngeal carcinoma. Int J Otolaryngol. 2011;2011:638058.
30. Xiao-Ping Y, Jing H, Fei-Ping L, Yin H, Qiang L, Lanlan W, Wei W. Intravoxel incoherent motion MRI for predicting early response to induction chemotherapy and chemoradiotherapy in patients with nasopharyngeal carcinoma. J Magn Reson Imaging 2016;43(5):1179–90.
31. Xiao YP, Pan JJ, Chen YB, Chen Y, He ZZ, Zhang X. Intravoxel incoherent motion-magnetic resonance imaging as an early predictor of treatment response to neoadjuvant chemotherapy in locoregionally advanced nasopharyngeal carcinoma. Medicine (Baltimore) 2015;94(24):e973.
32. Zheng D, Chen Y, Liu X, Chen Y, Xu L, Ren W, Chen W, Chan Q. Early response to chemoradiotherapy for nasopharyngeal carcinoma treatment: Value of dynamic contrast-enhanced 3.0 T MRI. J Magn Reson Imaging 2015;46(6):1528–40.
33. Zheng DC, Yue QY, Ren W, Liu M, Zhang XX, Lin H, Lai GJ, Chen WB, Chan QN, Chen YB. Early responses assessment of neoadjuvant chemotherapy in nasopharyngeal carcinoma by serial dynamic contrast-enhanced MR imaging. Magn Reson Imaging 2017;35:125–31.
34. Zheng D, Chen Y, Chen Y, Xu L, Lin F, Lin J, Huang C, Pan J. Early assessment of induction chemotherapy response of nasopharyngeal carcinoma by pretreatment diffusion-weighted magnetic resonance imaging. J Comput Assist Tomogr. 2013;37(5):673–80.
35. Chen Y, Liu X, Zheng D, Xu L, Hong L, Xu Y, Pan J. Diffusion-weighted magnetic resonance imaging for early response assessment of chemoradiotherapy in patients with nasopharyngeal carcinoma. Magn Reson Imaging 2014;32(6):630–7.
36. Li H, Zhu Y, Burnside ES, Drukker K, Hoadley KA, Fan C, Conzen S, Whitman GJ, Sutton EJ, Net JM, Ganott M, Huang E, Morris EA, Perou CM, Ji Y, Giger M. MR imaging radiomics signatures for predicting the risk of breast cancer recurrence as given by research versions of MammaPrint, oncotype DX, and PAM50 gene assays. Radiology 2016;281(2):382–91.
37. Zhao L, Gong J, Xi YB, Xu M, Li C, Kang XW, Yin YT, Qin W, Yin H, Shi M. MRI-based radiomics omogram may predict the response to induction chemotherapy and survival in locally advanced nasopharyngeal carcinoma. Eur Radiol. 2020;30(1):537–46.
38. Castellano G, Bonilha L, Li LM, Cendes F. Texture analysis of medical images. Clin Radiol. 2004;59(12):1061–9.
39. Ganeshan B, Goh V, Mandeville H, Ng QS, Hoskin PJ, Miles KA. Non-small cell lung cancer: Histopathological correlates for texture parameters at CT. Radiology 2013;266(1):326–36.
40. Ng F, Kozarski R, Ganeshan B, Goh V. Assessment of tumor heterogeneity by CT texture analysis: Can the largest cross-sectional area be used as an alternative to whole tumor analysis? Eur J Radiol. 2013;82(2):342–8.
41. Lubner MG, Stabo N, Lubner SJ, del Rio AM, Song C, Halber RB, Pickhardt PJ. CT textural analysis of hepatic metastatic colorectal cancer: Pre-treatment tumor heterogeneity correlates with pathology and clinical outcomes. Abdom Imaging 2015;40(7):2331–7.